

Asteroseismic signatures of the helium-core flash

M. M. Miller Bertolami*, T. Battich, A. H. Córscico,
J. Christensen-Dalsgaard, L. G. Althaus

August 2019

Letter to *Nature Astronomy*

All evolved stars with masses $M_* \lesssim 2M_\odot$ undergo a helium(He)-core flash at the end of their first stage as a giant star. Although theoretically predicted more than 50 years ago[1, 2], this core-flash phase has yet to be observationally probed. We show here that gravity modes (g modes) stochastically excited by He-flash driven convection are able to reach the stellar surface, and induce periodic photometric variabilities in hot-subdwarf stars with amplitudes of the order of a few mmag. As such they can now be detected by space-based photometry with the Transiting Exoplanet Survey Satellite (TESS) in relatively bright stars (e.g. magnitudes $I_C \lesssim 13$)[3]. The range of predicted periods spans from a few thousand seconds to tens of thousand seconds, depending on the details of the excitation region. In addition, we find that stochastically excited pulsations reproduce the pulsations observed in a couple of He-rich hot subdwarf stars. These stars, and in particular the future TESS target Feige 46, are the most promising candidates to probe the He-core flash for the first time.

After the end of their adult lives burning hydrogen (H) in the core, low-mass stars (up to about $2M_\odot$) evolve into the Red Giant Branch (RGB), where they develop a He core surrounded by a H-burning shell. Due to the high densities, the structure of the He-core is supported by the pressure of degenerate electrons. As H burning proceeds, the mass of the He core

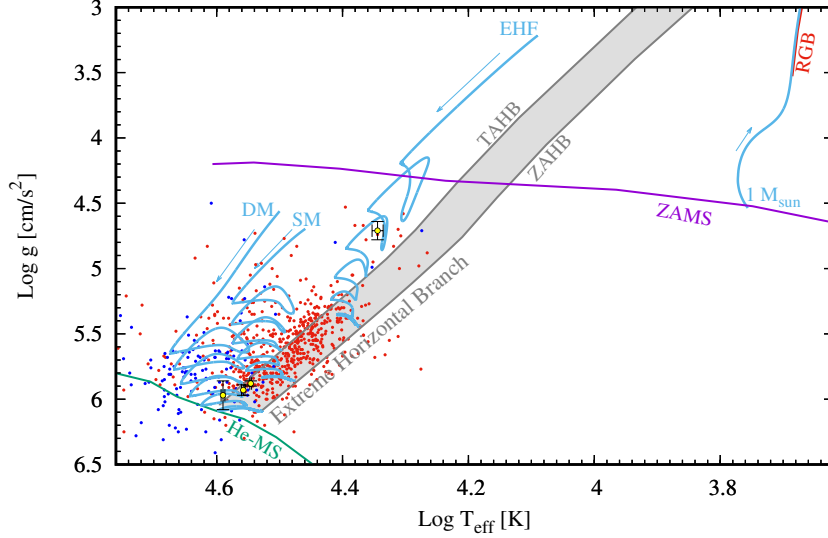


Figure 1: **Locus of hot subdwarfs in a $\log T_{\text{eff}} - \log g$ diagram.** Red and blue dots indicate the positions of spectroscopically analysed hot H- and He-rich subdwarfs respectively[4]. The He-rich hot-subdwarf pulsators studied in this work are shown as yellow circles with black errorbars. Errorbars correspond to the formal fitting errors reported by each author[41, 42, 43, 44]. Hot subdwarf stars are located at the hottest end ($\log T_{\text{eff}} \gtrsim 4.3$) of the horizontal branch (HB), bounded by the Zero Age Horizontal Branch (ZAHB) and Terminal Age Horizontal Branch (TAHB) shown with black lines[9]. For the sake of clarity the Zero Age Main Sequence of H-burning stars (ZAMS) and the Zero Age He Main Sequence formed by pure He-stars are shown with purple and green lines respectively[10]. The red giant branch (RGB) is shown with a red line. The evolutionary tracks of model stars before the ZAHB (i.e. the pre-HB stage) are shown in blue[40]. Blue labels indicate the location of our Early Hot-Flasher (EHF), Shallow Mixing (SM) and Deep Mixing (DM) models during the He subflashes (with initial abundances $(X_{\text{ZAMS}}, Y_{\text{ZAMS}}, Z_{\text{ZAMS}}) = (0.695, 0.285, 0.02)$). Also shown is the beginning of the evolution of a $1M_{\odot}$ main sequence star. All theoretical sequences and tracks correspond to models with metallicity $Z_{\text{ZAMS}} = 0.02$. Arrows indicate the sense of evolution.

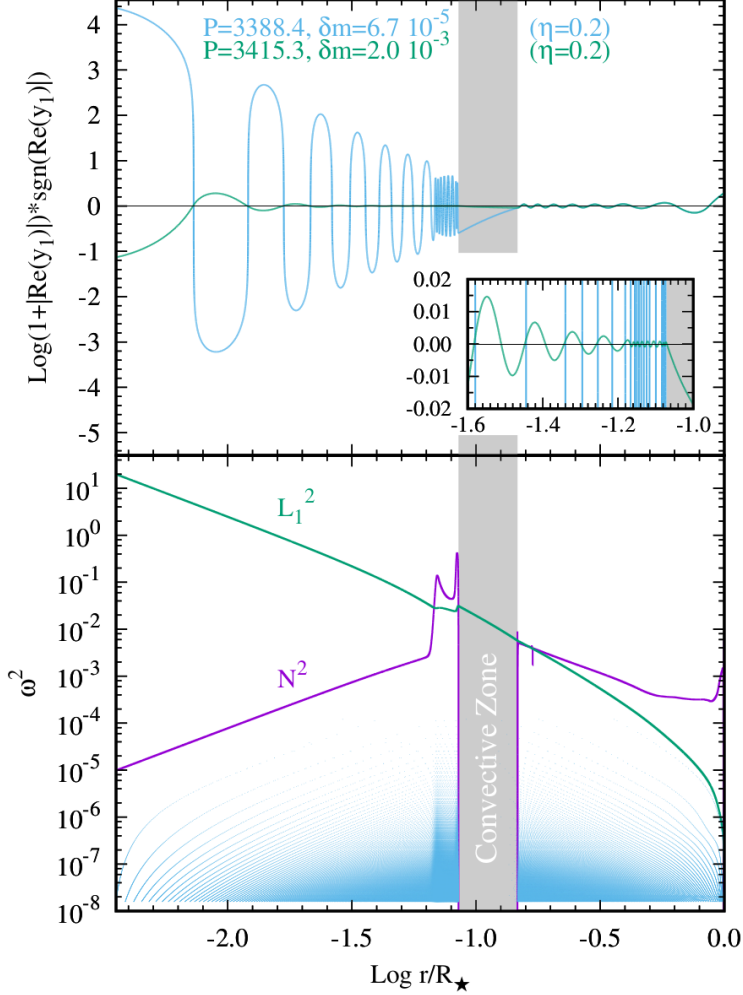


Figure 2: **Propagation diagram and pulsation eigenfunctions for $\ell = 1$ modes in a pre-EHB stellar model during a He subflash.** Lower panel: Squared Lamb (L_1^2) and Brunt-Vaisälä (N^2) frequencies together with the location of radial nodes (light-blue dots) for computed eigenfunctions at different angular eigenfrequencies ω^2 . Upper panel: Magnitude of the radial displacement eigenfunctions [45] y_1 of two consecutive radial orders and similar periods (P), but with very different global properties and predicted pulsation amplitudes (δm). Note that eigenfunctions in the linear pulsation theory are arbitrarily set to $|y_1| = 1$ at the surface and, consequently only relative differences are physically meaningful. The grey band displays the location of the convective zone driven by the He flash. The model shown in this figure corresponds to the maximum energy release by the He flash during the first subflash of the DM sequence shown in figure 1.

increases and so does its temperature. Eventually, this process leads to a violent ignition of He in the core, which is termed the He-core flash. Owing to the neutrino cooling of the central regions, the initial ignition takes place at some distance from the centre of the core. This first He flash, where the He-burning power reaches $L_{\text{He}} \gtrsim 10^{10} L_{\odot}$, is followed by a series of subflashes progressively deeper in the core. This phase lasts for about 2 Myr until degeneracy is lifted and steady He-core burning can start[10]. He-core burning stars populate the so-called Red Clump and the Horizontal Branch (HB) in the Hertzsprung-Russell diagram[13] (see figure 1).

Due to the inherent difficulty of gathering direct information from the core of stars, the He flash and its subflashes have remained unprobed for almost 60 years. In the last decades, and with the advent of space observatories like *Kepler*[14] and *CoRoT*[15], the use of stellar pulsations to learn about the interior of stars, a technique known as asteroseismology, has grown to become one of the most flourishing fields in stellar astrophysics. This is particularly true in the case of solar-like (stochastically excited) pulsators. In these stars, the bubbling motions in the convective envelope shake the star as a whole, globally exciting a discrete spectrum of eigenmodes. The excited eigenmodes are intrinsically damped by heat loss, so that the pulsations reach an equilibrium amplitude in which the energy injected by convective motions is balanced by the energy lost as heat by each mode. The unprecedented quality of the lightcurves from space missions has allowed the identification of a large number of modes, in solar-like pulsators. While most pulsations observed in solar-like pulsators are pressure modes (p modes), where the main restoring force are pressure gradients, some solar-like pulsators exhibit stochastically excited gravity modes (g modes)[16]. Gravity modes are oscillation modes where the primary restoring force is gravity, through buoyancy. Gravity modes are usually able to penetrate deeper in the star than p modes. As a consequence, g modes are extremely useful to constrain the internal structure of stars, and it has been speculated that the He-core flash could produce such signals in the pulsation spectrum of RGB stars[17, 18].

We present here compelling evidence that g-mode pulsations can be excited to observable levels by the inner convective zone driven by He-core flashes. Previous work[19] has shown that the convective energy injected into p (F_p) and g modes (F_g) scales as $F_p \propto M_c^{15/2} F_c$ and $F_g \propto M_c F_c$, where F_c is the total convective energy flux and M_c the Mach number of convective mo-

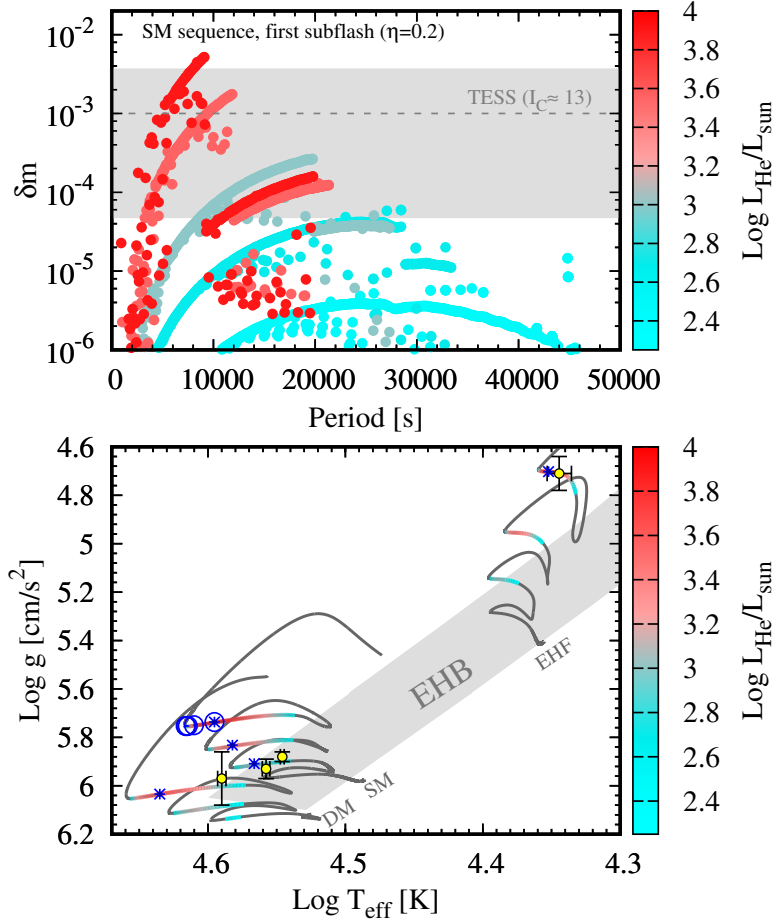


Figure 3: **Evolution of T_{eff} , g and L_{He} in our stellar models and development of pulsations as compared with known He-rich subdwarf pulsators.** Lower panel: $T_{\text{eff}}-g$ diagram of our computed DM, SM and EHF sequences for an initially He-enhanced population $(X_{\text{ZAMS}}, Y_{\text{ZAMS}}, Z_{\text{ZAMS}}) = (0.58, 0.40, 0.02)$ as compared with the known pulsating He-sdOBs shown as yellow points with black error bars [41, 42, 43, 44] (from left to right UVO 0825+15, Feige 46, LSIV -14°116, and KIC 1718290). Errorbars correspond to the formal fitting errors reported by each author. Colours indicate the He-burning luminosity in the parts of the evolution in which models harbour an internal convective zone. Blue circles in the SM sequence indicate the models described in the upper panel and blue asterisks models described in figure 4 and in the supplementary material. Upper panel: Evolution of the predicted pulsation amplitudes of $\ell = 1$ g modes during the development of the first subflash in the SM sequence shown in the lower panel (open blue circles). Colours indicate the He-burning luminosity in each model. The gray band indicates the typical range of amplitudes observed in He-sdBs while the dash line indicates the expected sensitivity limit for TESS for a star with $I_C \simeq 13$.

tions — $M_c = v_c/c_{\text{sound}}$, with v_c the typical velocity of convective motions and c_{sound} the sound speed. With values of $M_c \ll 1$, inner convective zones are unable to excite p modes to observable amplitudes, but the situation is more favourable for g modes. Still, even in massive stars with intense core-H burning the total convective flux in the core is only able to excite pulsations with very low amplitudes ($10\mu\text{mag}$)[20] because oscillations are strongly damped in their massive radiative envelopes. Fortunately, a much more favourable situation takes place during the He flash of low-mass stars that will populate the hot extreme of the horizontal branch (EHB, $M_{\star}^{\text{EHB}} \simeq 0.5M_{\odot}$), known as hot subdwarfs[21] (sdO and sdB spectral types). In these pre-EHB stars, the He-burning luminosity (L_{He}) reaches values of $L_{\text{He}} \gtrsim 10^4 L_{\odot}$ during the subflashes, and the mass of the radiative damping zone on top of the convective zone is significantly smaller. Also, the mass of the star is one order of magnitude lower and easier to disturb than that of more massive stars. In addition, the sdBs and sdOs have calm, stable atmospheres without convection or winds, making the surface imprint of non-radial oscillations easier to detect.

We have performed numerical simulations to compute the predicted amplitudes of stochastically driven $\ell = 1$ g modes in pre-EHB stars during the He subflashes in the framework of the hot-flasher scenario [22, 23, 24, 25, 26, 27]. Stellar evolution models have been constructed with LPCODE stellar evolution code from initially $1M_{\odot}$ stars with different initial He compositions[40]. Within this scenario sdB stars are formed when almost the whole H-rich envelope is stripped by winds during the RGB phase, and the He-core flash develops once the star has contracted away from the RGB[22]. Hot-flasher sequences are labeled as “early hot flashers” (EHF), “shallow mixing” (SM) or “deep mixing” (DM) as in previous works[25, 26, 40]. While in the case of the EHF flavour the sdB model retains its original H/He atmosphere, in the SM and DM cases the final surface composition is set by the action of mixing and burning immediately after the main He-core flash, leading to a He-enriched surface[26, 40]. Snapshots of the internal structure of these stars during the subflashes in the pre-EHB phase are then fed into the linear non-adiabatic pulsation code LP-PUL[28] for the computation of normal modes (see figure 2), their kinetic energies (E^{linear}) and the damping rates of the modes (γ) as determined by all non-adiabatic effects. However, linear pulsation analyses do not provide the actual amplitudes of the pulsations. Amplitudes are obtained from balancing the power injected by convection into g modes and the power lost due to non-adiabatic effects during the os-

cillations (see Methods). The convective energy flux F_c was computed in the framework of the mixing-length theory (MLT)[10], and the power spectrum of energy supplied by convection to g modes computed under the simplifying assumption that waves are excited by eddies and that the buoyancy frequency (N) can be treated as discontinuous at convective boundaries, as in previous work[19, 20] (see Methods). This model for gravity wave excitation[29] has been validated by numerical studies[30] and, despite important uncertainties in the predicted energy spectrum, can be considered a conservative estimation, as competing models predict larger gravity wave excitation[31], and the consideration of a smooth transition in the buoyancy frequency would also lead to an enhancement in the predicted excitation[29]. Following previous work[20], we parametrize the thickness of the excitation region close to the convective boundaries by including a parameter η , so that the geometrical size of the excitation region is ηH_P , where H_P is the local pressure scale height at the formal convective boundary. Values of the order of $\eta \sim 0.1$ are typical of convective boundary mixing under different circumstances from the main sequence to the asymptotic giant branch[32].

Our simulations show that stochastically excited oscillations can produce lightcurve variations of more than 1 mmag and even up to 10 mmag. As shown in figures 3 and 4 for the case of our $Y_{\text{ZAMS}} = 0.4$ models, this is similar to the pulsations detected in He-sdOBs stars and also well within the detectability range of TESS for bright subdwarf stars[3], e.g. with magnitudes $I_C \lesssim 13$, of which more than one hundred are known[4]. The predicted amplitudes are even larger in the case of our $Y=0.285$ sequences, for which the He-flashes are more intense (see supplementary material). In latter, less intense flashes, the excitation becomes less intense and amplitudes will be undetectable with current technology (figures 3 and 4). The longest excited periods are also the most excited, and correspond to the turn-over frequency of convective motions ($\omega_c(\eta)$) at the excitation region of size ηH_P (see Methods). This is a natural consequence of the fact that the energy transport by convection occurs mostly via the largest possible eddies. Consequently, the thinner the excitation region, the higher characteristic frequency by a factor $1/\eta$. This shifts the bulk of the g-mode power input to higher frequencies, increasing the amplitudes of high frequency g modes for thinner excitation regions. On the other hand, the characteristic frequency $\omega_c(\eta)$ beyond which no pulsations are excited is also decreased by the same factor. Our computations show that not all eigenmodes are excited to the same amplitude. Eigenmodes that oscillate mostly in the outer parts of the star have lower

inertia and are more easily excited by convection, and therefore have larger amplitudes (see figure 2). The range of predicted periods spans from a couple thousand seconds to tens of thousand seconds depending on the details of the excitation region and the compactness of the stellar model. This provides for the first time an extremely exciting prospect to probe the He-core flash and to explore the nature of convective boundary mixing in He flashes by asteroseismological means.

Given the large number of known hot subdwarfs[4] ($N > 5000$) and given that the pre-horizontal branch evolution lasts for about 2Myr ($\sim 2\%$ of the total He-core burning lifetime) we may expect that some of known hot subdwarfs are in the pre-HB evolution. In particular, He-rich hot subdwarfs (He-sdO/He-sdB spectral types) are natural candidates, as the low surface abundance of H suggests that these stars are in a fast evolutionary stage, where H has not had enough time to diffuse and form a pure H atmosphere[26, 33]. Pre-EHB model sequences spend 0.5 to 1% of their pre-EHB stage having high He-burning luminosities $L_{\text{He}} \gtrsim 10^3 L_{\odot}$ and thus a similar fraction of stars should display detectable stochastic oscillations, see figure 3. Notably, four He-rich hot-subdwarfs (out of ~ 500 He-rich subdwarfs known[4]) are known to pulsate, the pulsation mechanism being still matter of debate[40, 34, 42, 43, 44, 35]. Noteworthy, the locus of these stars in the $\log g - \log T_{\text{eff}}$ diagram overlaps with that of pre-EHB model sequences during the He subflashes, see figures 1 and 3.

In figure 4 we compare the range of periods excited in our models by convective motions with periods detected in the known He-rich subdwarf pulsators. Remarkably, our models show that stochastic excitation during the He-core flash is able to excite periods in the range observed in He-rich subdwarfs for excitation regions with sizes typical of overshooting zones in stellar evolution (i.e. $\eta \simeq 0.1 \dots 0.3$). The ranges of amplitudes and periods measured in the twin stars LS IV -14°116 and Feige 46 are well reproduced by our SM models with enhanced initial He abundances ($Y = 0.4$) in which the excitation takes place in a thin region of size $\sim 0.1 H_P$ (see figure 4). This agreement is reinforced by the fact that this sequence also nicely reproduces the spectroscopical determinations of $\log T_{\text{eff}}$ and $\log g$ in these two stars (figure 3). On the other hand the large number of long periods observed in KIC 1718290 are also nicely reproduced by our EHF sequences with a thin excitation region ($\eta \sim 0.3$) which also nicely reproduces the $\log T_{\text{eff}}$ and $\log g$ values determined for this star. This is true for both our EHF sequences with $Y_{\text{ZAMS}} = 0.4$ and $Y_{\text{ZAMS}} = 0.25$, see figures 1, 3, 4 and the supplementary

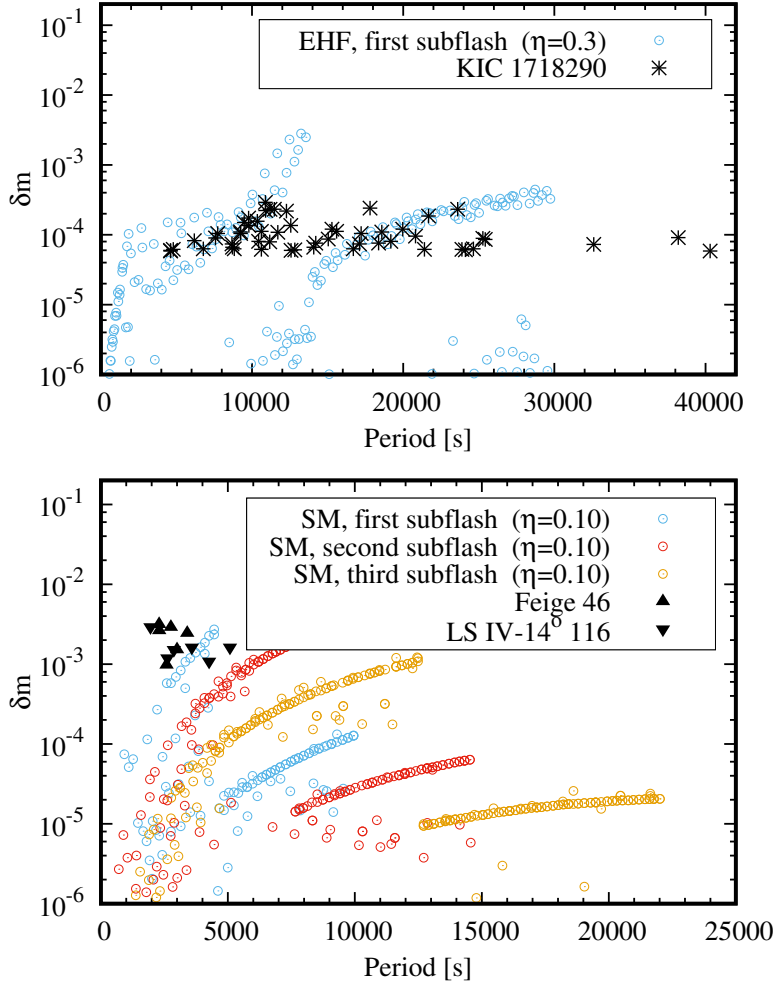


Figure 4: **Observed and predicted pulsation amplitudes of $\ell = 1$ g modes.** Comparison of the predicted maximum pulsation amplitudes $|\delta m|$ with the actual periods and pulsation amplitudes observed in the He-rich subdwarfs. Predicted amplitudes are shown for the models indicated in figure 3 with blue asterisks. Lower panel: Data from LS IV-14^o116, and Feige 46 and pulsation amplitudes predicted for our SM sequence ($Y_{\text{ZAMS}} = 0.4$) during the first three subflashes for $\eta = 0.1$. Upper panel: Data from KIC 1718290, and pulsation amplitudes predicted for our EHF sequence ($Y_{\text{ZAMS}} = 0.4$) during the first subflashes for $\eta = 0.3$.

material. Although the longest modes are not reproduced, this can be easily accommodated by a slightly larger choice of η . On the contrary, the very long and isolated pulsation modes observed in UVO 0825+15[43] cannot be reproduced by our sequences. While a choice of $\eta \sim 1$ would lead to the excitation of those modes, such excitation would be accompanied with the excitation of a range of shorter periods (as those observed in KIC 1718290) that are not observed in this star. In addition, a choice of $\eta \sim 1$ is incompatible with the choices made in our model, most importantly with the assumption of a discontinuous buoyancy frequency at convective boundaries, and with the use of the frozen convection approximation (see Methods). Consequently, we conclude that the stochastic excitation of pulsations provides a natural explanation for the lightcurves observed in KIC 1718290, LSIV -14°116, and Feige 46 all of which lack another plausible explanation, but that they are unable to explain the lightcurve observed in UVO 0825+15.

Our computations show that new space observatories, such as TESS, allow us to search for direct asteroseismological signatures of the He-core flash phase in hot subdwarf stars. This is particularly true in the case of Feige 46 which has already been scheduled as TESS target[44]. One of the distinctive features of a star evolving through this very fast evolutionary stage would be a large rate of period drift[40] $\dot{P} \sim 10^{-7}-10^{-4}$ s/s. The determination of such large rates of period drift in a pulsating hot subdwarf would be a smoking gun for the He-core flash phase.

Methods

La Plata stellar evolution code

All stellar evolution models presented in this work have been computed with LPCODE, a one-dimensional stellar evolution code that has been widely used for the computation of full evolutionary sequences from the zero age main sequence to the white dwarf stage. The last version of LPCODE includes a state-of-the-art treatment of atomic, molecular and conductive opacities as well as a detailed treatment of stellar winds and convective boundary mixing[32, 36, 37].

Models of He-rich hot subdwarfs were constructed within the hot-flashers scenario as in our previous work[40]. Models were calculated from the evolution of initially $1M_{\odot}$ models on the Zero Age Main Sequence (ZAMS) to the end of the RGB where the He-core flash develops. At the tip of the RGB we switched on artificially enhanced mass loss, removing different amounts of envelope mass to obtain the different types of hot-flasher sequences. For the purpose of this work, the particular value of the mass at the ZAMS and the treatment of mass loss at RGB are not relevant, since it is the total envelope mass at He ignition that determines the behaviour of the hot flashers.

La Plata stellar pulsation code

Normal oscillation modes and theoretical pulsation periods have been computed with the non-adiabatic version of LP-PUL[28]. LP-PUL is a linear, non-radial, non-adiabatic stellar pulsation code, which is coupled to the LPCODE. The LP-PUL was widely used in studies of pulsation properties of late stages of low-mass stars. In particular it was recently used by our group to study the excitation of pulsations by means of the ϵ mechanism in hot pre-HB stars[40]. LP-PUL allows as to compute the damping rates of the oscillation modes (γ) in the full non-adiabatic regime as well as the kinetic energies of the modes $E^{\text{linear}}(\omega, \ell)$ under the standard normalization[45] ($\xi_{R_{\star}}/R_{\star} = 1$, see below). Non-adiabatic computations in this work rely on the frozen-in convection approximation, in which the perturbation to the convective flux is neglected, an approximation that breaks down for modes with periods similar or longer than the convective turn-over timescale.

Computation of stochastically excited pulsations

To compute the predicted maximum luminosity variations due to the excited modes, we follow the approach of previous work[20]. Specifically, we compute the equilibrium energy $E_{mode}^{eq}(\omega, \ell)$ of the excited modes by equating the energy injected by convection and the energy dissipated by non-adiabatic effects,

$$E_{mode}^{eq}(\omega, \ell) = \frac{1}{2} \frac{d\dot{E}_g}{d \ln \omega d\ell} N(\omega, \ell)^{-1} \gamma^{-1} \quad (1)$$

where $N(\omega, \ell) \simeq (n + \ell/2)(2\ell + 1)$ is the number of modes in a logarithmic bin in ω (for a given ℓ), γ is the damping rate of the mode due to non-adiabatic effects, and $d\dot{E}_g/d \ln \omega d\ell$ is the power spectrum of energy supplied by convective motions to the g modes.

We compute γ within the non-adiabatic linear oscillation theory with LP-PUL[28] and estimate the power spectrum supplied by convective motions under the assumption that the excitation occurs at the edge of the convective boundaries, under the approximation of a discontinuity in the buoyancy frequency at the radiative-convective transition, as in previous work[19, 20],

$$\begin{aligned} \frac{d\dot{E}_g}{d \ln \omega d\ell} &= BM_c L_{conv} \\ &\times \left(\frac{\omega}{\omega_c} \right)^{-13/2} \ell^2 \left(\frac{\eta H_P}{r} \right)^3 \left(1 + \ell \frac{\eta H_P}{r} \right) \exp \left[- \left(\frac{\ell}{\ell_{max}} \right)^2 \right] \end{aligned} \quad (2)$$

which is valid over the range $\omega \geq \omega_c = v_{MLT}/(\eta H_P)$, and $\ell \gtrsim 1$. L_{conv} is the total power carried by convection, H_P is the pressure scale height, v_{MLT} is the convective velocity, $M_c = v_{MLT}/c_{sound}$ is the convective Mach number, ω_c is the convective turn-over frequency, $\ell_{max} = (r/\eta H_P)(\omega/\omega_c)^{3/2}$, and both H_P and r are evaluated at the convective boundaries. Convective velocities and luminosities are taken as a mean value in the excitation region of size $0.2H_P$ next to the formal convective boundary. It is worth noting that, as the flash-driven convective zone has two convective boundaries (figure 2), the total energy received by each mode is given by the sum of the energies provided by the two convective boundaries (E_g^{inf} and E_g^{sup}), i.e.

$$\frac{d\dot{E}_g}{d \ln \omega d\ell} = \frac{d\dot{E}_g^{inf}}{d \ln \omega d\ell} + \frac{d\dot{E}_g^{sup}}{d \ln \omega d\ell} \quad (3)$$

where both $d \ln \dot{E}_g^{\text{inf}} / d \ln \omega d \ell$ and $d \ln \dot{E}_g^{\text{sup}} / d \ln \omega d \ell$ are computed from equation 2 with the corresponding value of H_P .

Convective velocities and luminosities were computed with the help of the mixing-length theory [38] as

$$v_{\text{MLT}} = \left(\alpha_{\text{MLT}} \frac{acG}{3} \frac{m}{r^2 \kappa \rho} \frac{T^4}{P} \nabla_{\text{ad}} (\nabla_{\text{rad}} - \nabla) \right)^{1/3} \quad (4)$$

and

$$L_{\text{conv}} = \frac{16ac\pi}{3} \frac{GmT^4}{\kappa P} (\nabla_{\text{rad}} - \nabla) \quad (5)$$

where all the quantities have the same meaning as in the classic textbook by Kippenhahn et al.[10].

In the linear stellar oscillation theory, the amplitudes of the eigenfunctions are arbitrary and are usually normalized by choosing $\xi_r(R_\star) = \delta r(r = R_\star) = R_\star$. As a consequence, the mode energies computed within the linear theory $E^{\text{linear}}(\omega, \ell)$,

$$E^{\text{linear}}(\omega, \ell) = \omega^2 / 2 \int_0^{M_\star} [\xi_r^2 + \Lambda(\omega, \ell)^2 \xi_h^2] \rho r^2 dr \quad (6)$$

differ from the equilibrium energy $E_{\text{mode}}^{\text{eq}}(\omega, \ell)$ by a constant $A(\omega, \ell)^2$. By comparing the energies computed in eqs. 1 and 6 we can derive $A(\omega, \ell)$ and normalize the linear eigenfunctions to obtain realistic predictions for the temperature, pressure, flux and radial perturbations (δT , δP , and δr).

Once the realistic surface perturbations were obtained, following the work by Dziembowski[39] we computed the instantaneous disk-averaged magnitude variations produced by the stochastically excited g modes as

$$\delta m = 1.086 \left(b_\ell \frac{\delta F(t, r, \theta_0, \phi_0)}{F} + (2b_\ell - c_\ell) \frac{\xi_r(t, r, \theta_0, \phi_0)}{R} \right)_{r=R_\star} \quad (7)$$

where in this expression the perturbations of flux $\delta F(t, r, \theta_0, \phi_0)$ and radius $\xi_r(t, r, \theta_0, \phi_0)$ depend of the direction to the observer (θ_0, ϕ_0) and time t . From equation 7, we can then derive the amplitude of the lightcurve of each mode as

$$|\delta m| = 1.086 \sqrt{(b_\ell \Re(y_6) - c_\ell \Re(y_1))^2 + (b_\ell \Im(y_6))^2} \times A(\omega, \ell), \quad (8)$$

where the factor $A(\omega, \ell)$ renormalizes the y_1 and y_6 coming from the LP-PUL (which defines $y_1(R_\star) = 1$ [45]) to their physical value. In equation 8, \Re and

\Im denote the real and imaginary parts of the eigenfunctions y_1 and y_6 , which are defined as

$$y_1 = \xi_r/r, \quad y_6 = \delta L_r/L_r \quad (9)$$

where $\delta L_r = 4\pi r^2(\delta F_r + 2F_r \xi_r/r)$ and, under the assumption of no convection in that particular region (which is our case in the outer regions of a hot star) we have $L_r = 4\pi r^2 F_r^R$, and we can write

$$\frac{\delta F_r}{F_r} = \frac{\delta L_r}{L_r} - 2\frac{\xi_r}{r} = y_6 - 2y_1. \quad (10)$$

Equation 8 allows us to compute the maximum predicted amplitude for each normal mode (i.e. for the most favourable orientation θ_0, ϕ_0).

Code availability

The LPCODE and LP-PUL codes used in this paper are available under request from M.M.M.B. and A.H.C., respectively. Note that LPCODE and LP-PUL are not suitably written for public distribution.

Data availability

The data that support the plots within this paper and other findings of this study are available from the corresponding author upon reasonable request.

Supplementary Information

Sequences with $Y_{\text{ZAMS}} = 0.285$

Supplementary figures 5 and 6 show the same information as figures 3 and 4 of the main text but for our sequences with a standard initial He abundance of $Y_{\text{ZAMS}} = 0.285$. These sequences harbour larger He cores, and as a consequence undergo more intense He subflashes than the $Y_{\text{ZAMS}} = 0.4$ sequences of figures 3 and 4 in the main text. Note the difference in the range of the colour bars in figure 3 of the main text and supplementary figure 5 here. As a consequence these sequences also predict larger amplitudes due to stochastic excitation at the convective boundaries. However, as already noted by Battich et al.[40] these sequences do evolve at lower surface gravities due to their higher luminosity and, consequently the SM and DM tracks do not overlap during the first thermal pulses with the location of LS IV -14°116, and UVO 0825+15 (supplementary figure 5), and are consequently not favoured as models for these stars. On the contrary the $Y_{\text{ZAMS}} = 0.285$ EHF sequence does go through the location of KIC 1718290 and, in particular overlaps its location during the second He subflash. Interestingly during this second flash the models predict the excitation of g modes in the right range of periods and amplitudes (supplementary figure 6). We conclude that this sequence offers also a viable model for KIC 1718290 and its observed behaviour.

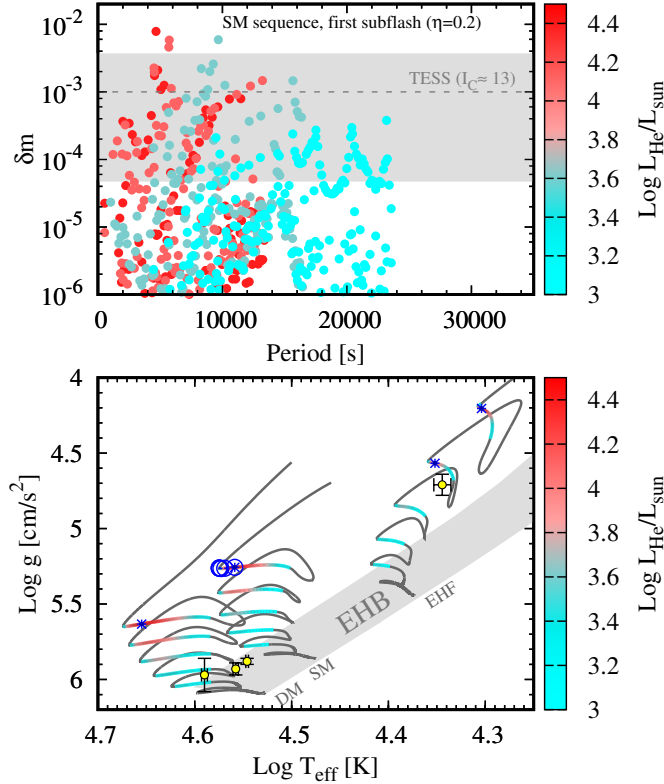


Figure 5: **Evolution of T_{eff} , g and L_{He} in our stellar models and development of pulsations as compared with known He-rich subdwarf pulsators.** Lower panel: $T_{\text{eff}}-g$ diagram of our computed DM, SM and EHF sequences for an initially He-enhanced population $(X_{\text{ZAMS}}, Y_{\text{ZAMS}}, Z_{\text{ZAMS}}) = (0.695, 0.285, 0.02)$ as compared with the known pulsating He-sdOBs shown as yellow points with black error bars (from left to right UVO 0825+15, Feige 46, LS IV -14° 116, and KIC 1718290). Errorbars correspond to the formal fitting errors provided by each author[41, 42, 43, 44]. Colours indicate the He-burning luminosity in the parts of the evolution in which models harbour an internal convective zone. Blue circles in the SM sequence indicate the models described in the upper panel and blue asterisks models described in figure 4 of the main text and in figures 6, 7, and 9. Upper panel: Evolution of the predicted pulsation amplitudes of $\ell = 1$ g modes during the development of the first subflash in the SM sequence shown in the lower panel (open blue circles). Colours indicate the He-burning luminosity in each model. The gray band indicates the typical range of amplitudes observed in He-sdBs while the dash line indicates the expected sensitivity limit for TESS for a star with $I_C \simeq 13$.

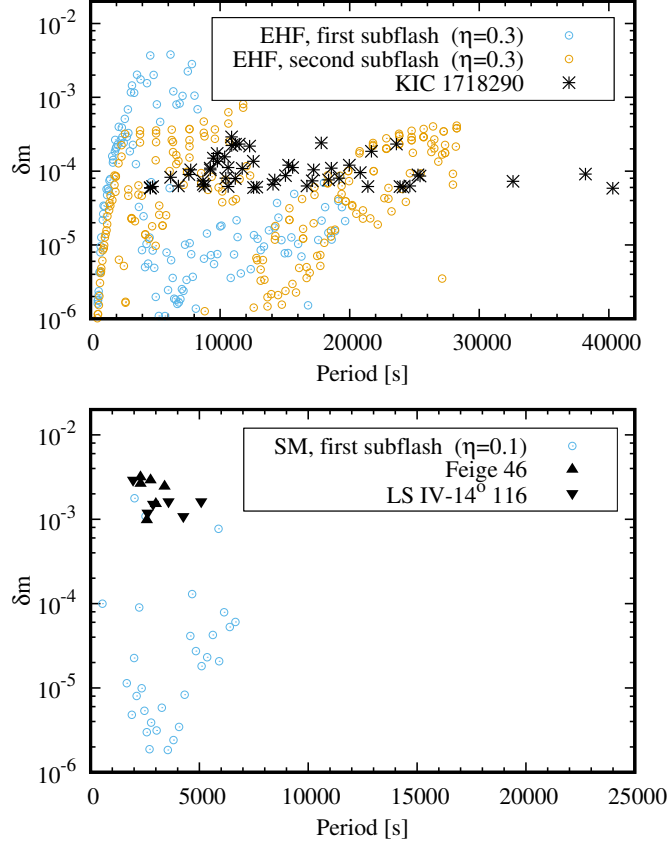


Figure 6: **Observed and predicted pulsation amplitudes of $\ell = 1$ g modes.** Comparison of the predicted maximum pulsation amplitudes $|\delta m|$ with the actual periods and pulsation amplitudes observed in the Herich subdwarfs. Predicted amplitudes are shown for the models indicated in figure 3 of the main text with blue asterisks. Lower panel: Data from LSIV-14°116, and Feige 46 and pulsation amplitudes predicted for our SM sequence ($Y_{\text{ZAMS}} = 0.285$) during the first three subflashes for $\eta = 0.1$. Upper panel: Data from KIC 1718290, and pulsation amplitudes predicted for our EHF sequence ($Y_{\text{ZAMS}} = 0.285$) during the first subflashes for $\eta = 0.3$.

UVO 0825+15

Supplementary figure 7 shows the observed periods in UVO 0825+15 compared with the excited modes in our DM sequences with $Y_{\text{ZAMS}} = 0.285$ (supplementary figure 5) and with $Y_{\text{ZAMS}} = 0.4$ (figure 3 of the main text). As is apparent from the figure, our models fail to reproduce the observed periods. Even when they manage to excite periods up to $P \gtrsim 40000\text{s}$ under the extreme assumption of $\eta = 1$, such models also predict a large range of shorter periods which are not observed in the star.

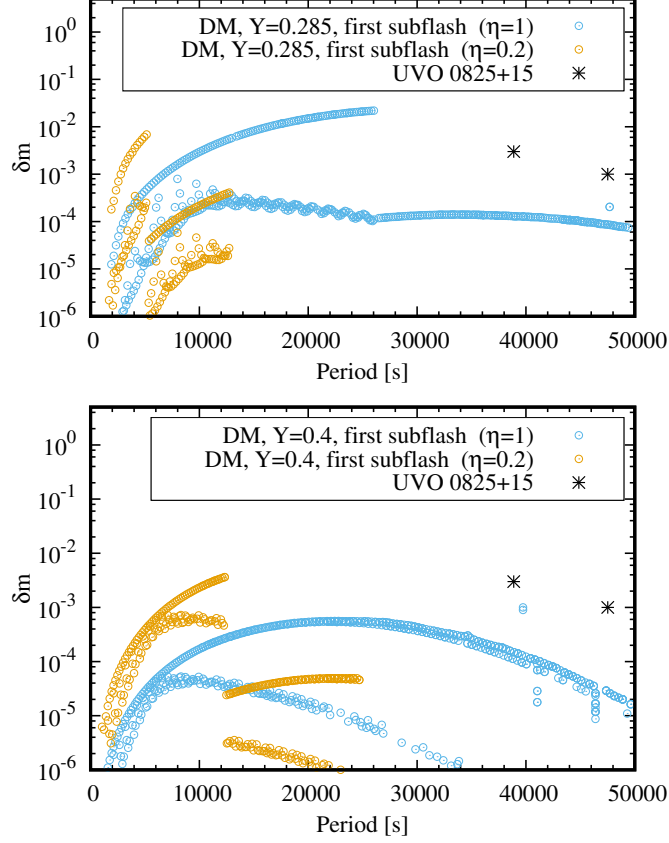


Figure 7: **Observed pulsation amplitudes observed in UVO 0825+15 as compared with the predicted amplitudes of $\ell = 1$ g modes in our DM sequences.** Lower panel: Comparison with our $Y_{\text{ZAMS}} = 0.4$ DM sequence for two different values of η . Upper panel: Comparison with our $Y_{\text{ZAMS}} = 0.285$ DM sequence for two different values of η .

Mode inertia and excitation at each convective boundary.

The first row in supplementary figures 9 and 10 show the maximum predicted amplitudes (δm) for stochastically excited pulsations for DM, SM and EHF models (first, second and third columns respectively) during the first subflash. As is apparent from these plots, two main families of modes arise, one with

amplitudes large enough to be observed ($\delta m \gtrsim 10^{-4}$) and a second one with very low amplitudes. The reason for this different behaviour can be traced to the different eigenfunctions of the modes. While modes with large amplitudes have eigenfunctions that show similar amplitudes in the core and in the envelope of the star (see upper panels in figure 2 of the main text and supplementary figure 8), modes with smaller amplitudes at the surface have eigenfunctions with very large amplitudes in the core. This leads to very different mode inertias (E^{linear} , second row in supplementary figures 9, 10, 11 and 12)¹ and damping rates (third row in supplementary figures 9, 10, 11 and 12) of the respective eigenmodes. Modes that are excited to larger amplitudes have unnormalized energies, E^{linear} , about five orders of magnitude lower than low amplitude modes. These large inertia modes have, however smaller damping rates γ by about 1 to 2 orders of magnitude (lower branch of modes in the third row of supplementary figures 9, 10, 11 and 12), which leads to equilibrium energies (second row in supplementary figures 9, 10, 11 and 12) only 1 to 2 orders of magnitude larger. In view of the large difference in the inertia of the modes of about 5 orders of magnitude these modes are excited to amplitudes much smaller than the low inertia modes.

Another interesting feature of our computations is that the lower convective boundary of the convective shell is the one providing most of the energy in our simulations (see second row of supplementary figures 9, 10, 11 and 12). This is due to the smaller spatial scales, which concentrates the energy injected into gravity waves and higher frequencies and the higher turbulent velocities at this convective boundary, larger Mach numbers, which lead to a larger total energy flux transferred to gravity waves.

¹Note that E^{linear} is a proxy for the inertia of the eigenmodes, as it indicates the total kinetic energy of the modes when the surface radial perturbation is $\xi_r(R_\star) = \delta r(r = R_\star) = R_\star$.

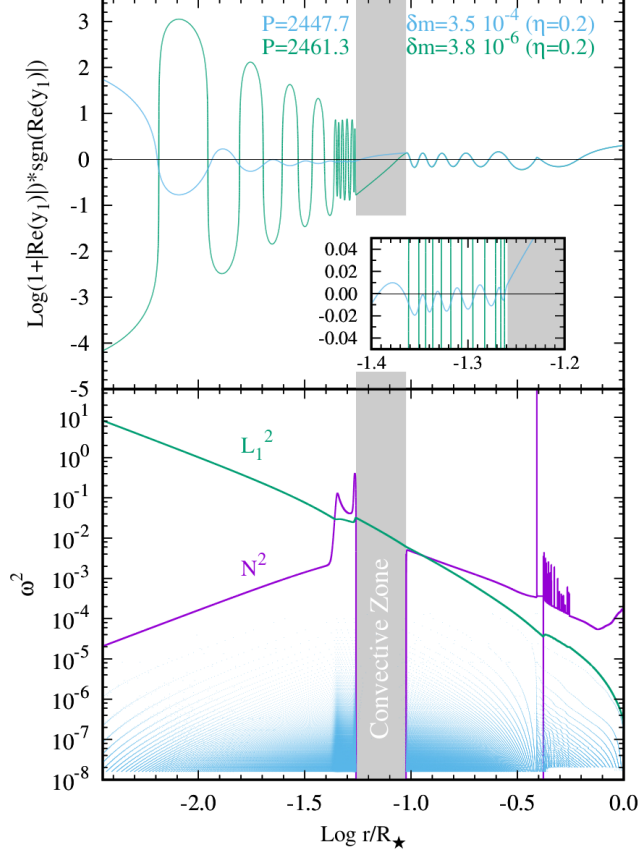


Figure 8: **Propagation diagram and pulsation eigenfunctions for $\ell = 1$ modes in a pre-EHB stellar model during a He subflash.** Lower panel: Squared Lamb (L_1^2) and Brunt-Vaisälä (N^2) frequencies together with the location of radial nodes (light-blue dots) for computed eigenfunctions at different angular eigenfrequencies ω^2 . Upper panel: Magnitude of the radial displacement eigenfunctions [45] y_1 of two consecutive radial orders and similar periods (P), but with very different global properties and predicted pulsation amplitudes (δm). Note that eigenfunctions in the linear pulsation theory are arbitrarily set to $|y_1| = 1$ at the surface and, consequently only relative differences are physically meaningful. The grey band displays the location of the convective zone driven by the He flash. The model shown in this figure corresponds to the maximum energy release by the He flash during the first subflash of the SM sequence shown in figure 1 of the main text ($Y_{\text{ZAMS}} = 0.285$).

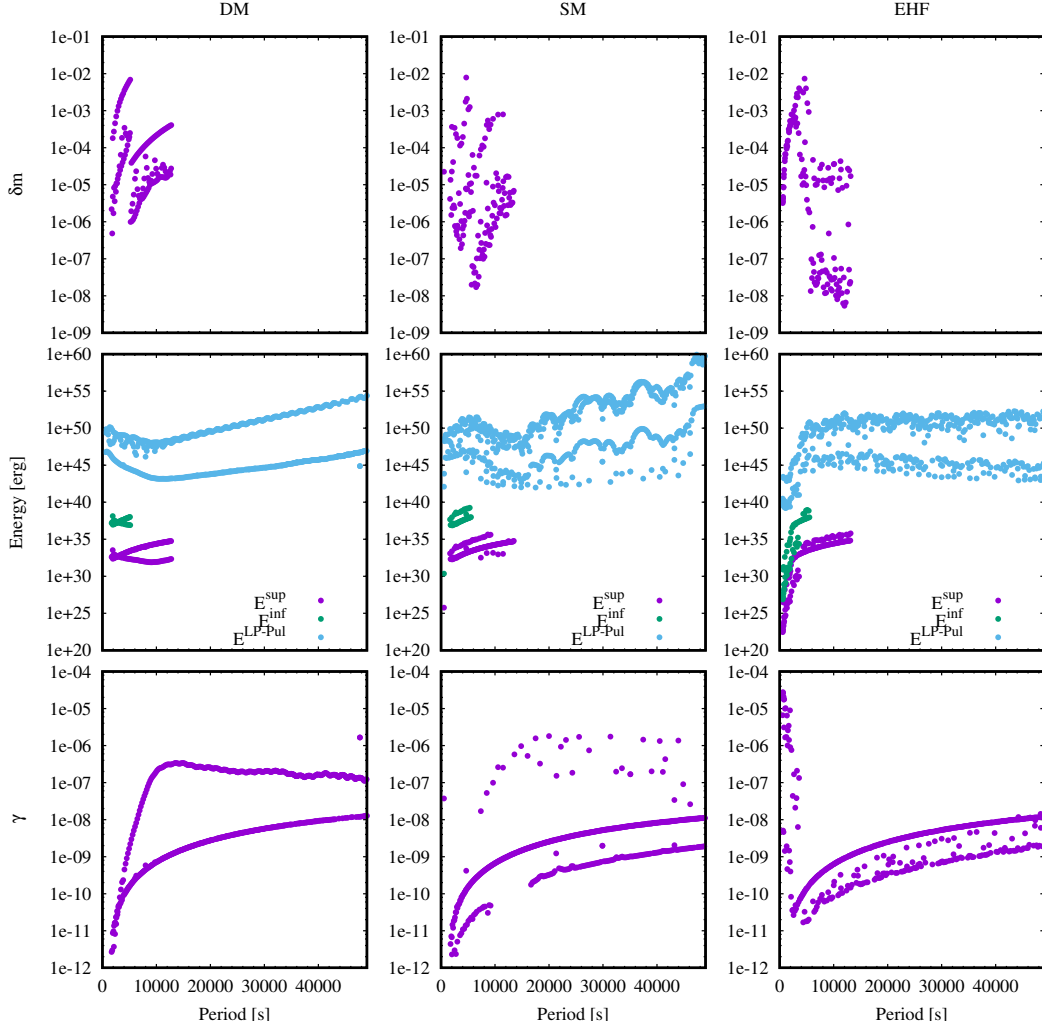


Figure 9: Pulsations properties of DM, SM and EHF models with canonical initial abundances ($Y = 0.285$) during the first subflash and under the assumption of $\eta = 0.2$. First, second, and third columns correspond to DM, SM and EHF models respectively. Top row shows the predicted pulsation amplitudes for eigenmodes at different periods. Middle row indicates the unnormalized energies, E^{linear} , computed by the linear pulsation code (LP-PUL) for all eigenmodes compared with the actual equilibrium energies derived from equation 1 (Methods section, main text) for the lower (E^{inf}) and upper (E^{sup}) convective boundaries of the He-flash driven convective zone. Bottom row shows the damping rates (γ) computed with LP-PUL for each eigenmode.

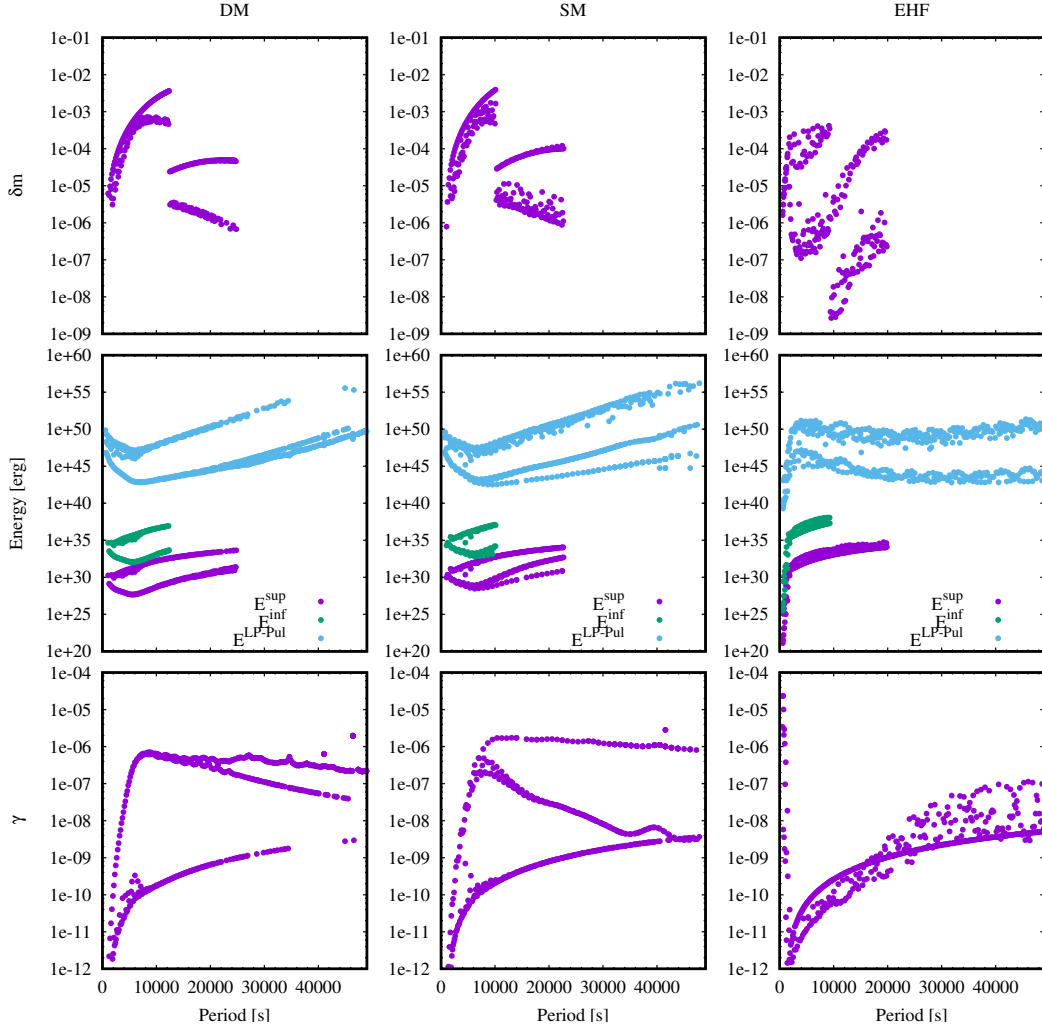


Figure 10: Pulsations properties of DM, SM and EHF models with He-enriched initial abundances ($Y = 0.4$) during the first subflash and under the assumption of $\eta = 0.2$. Rows and columns have the same meaning as in supplementary figure 9.

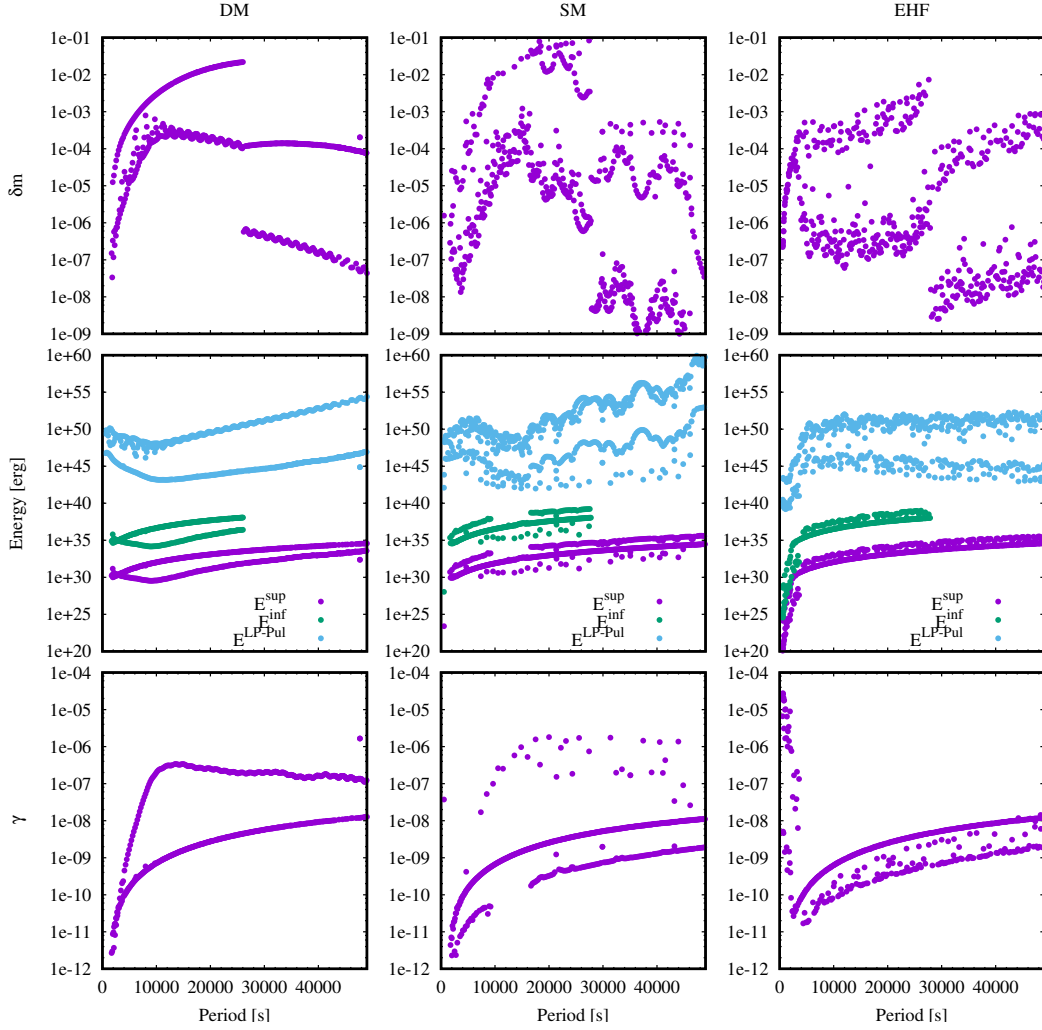


Figure 11: Pulsations properties of DM, SM and EHF models with canonical initial abundances ($Y = 0.285$) during the first subflash and under the assumption of $\eta = 1$. Rows and columns have the same meaning as in supplementary figure 9.

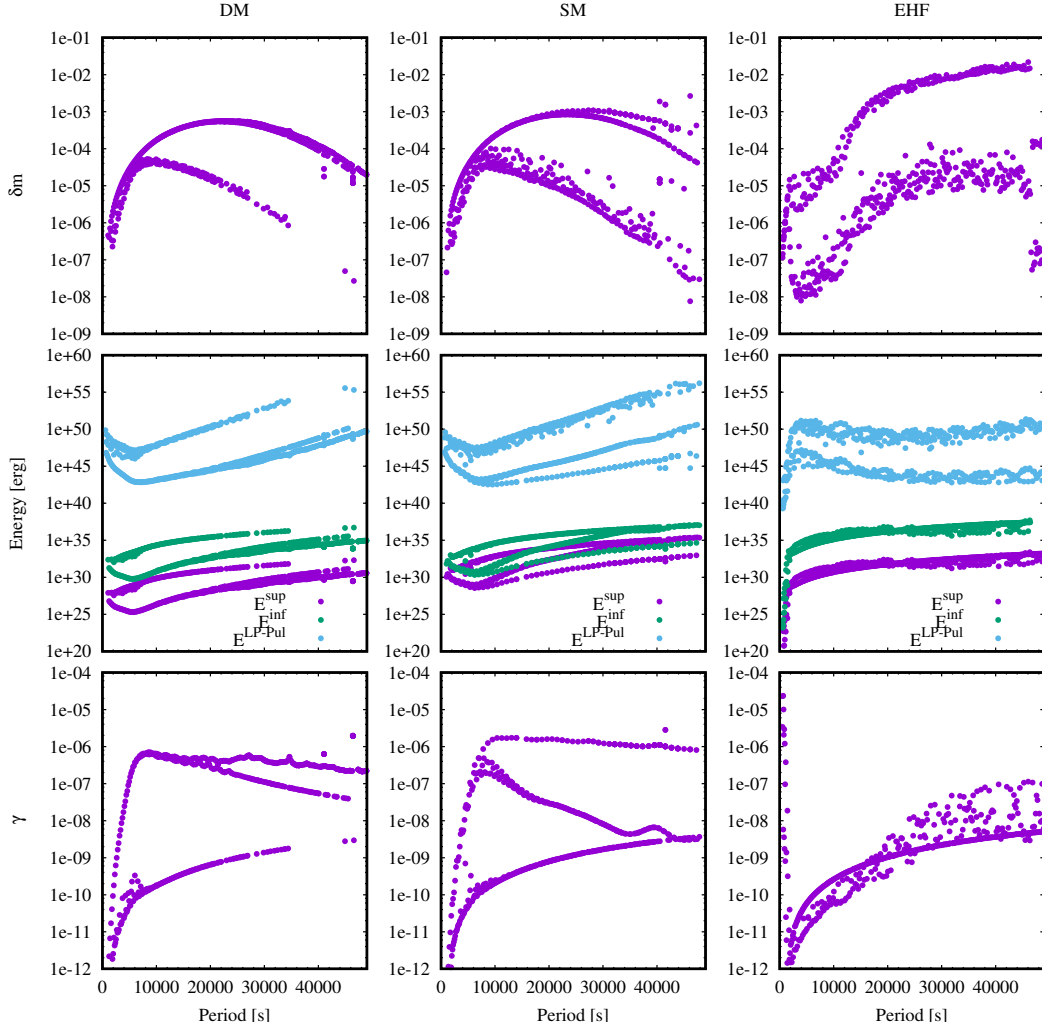


Figure 12: Pulsations properties of DM, SM and EHF models with He-enriched initial abundances ($Y = 0.4$) during the first subflash and under the assumption of $\eta = 1$. Rows and columns have the same meaning as in supplementary figure 9.

Numerical Resolution.

Spatial resolution is an important ingredient in this computations. Due to the very large radial order of the low frequency g modes a high spatial resolution is required. Modes with the longest periods computed in this work have more than 700 nodes and very complex eigenfunctions. For these reason all the models presented in this work have high density spatial grids between 13000 and 15000 mesh points. In addition we computed some sequences with extremely dense grids to test the stability of our solutions with numerical resolutions. Besides small differences due to the fact that the background stellar evolution models change slightly due to the high resolution grid, the qualitative results are very similar. High resolution and normal resolution computations both show the same two branches of low and high amplitude modes and a very similar behaviour of amplitude with period (supplementary figures 13 and 14). This shows that eigenfuctions are well resolved already at our normal resolution of about 13000 to 15000 mesh points.

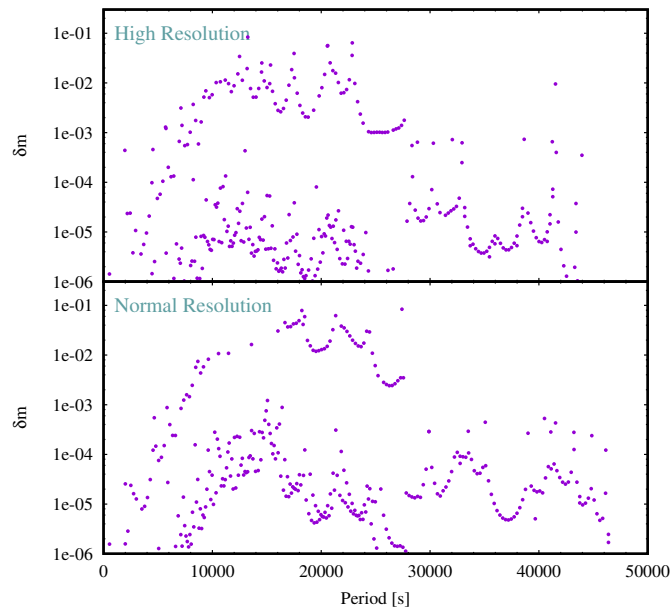


Figure 13: **Comparison of predicted amplitudes δm for SM models computed with different mesh resolutions.** The high resolution model was computed with 64330 mesh points and compared with the 14569 mesh points in the normal resolution run.

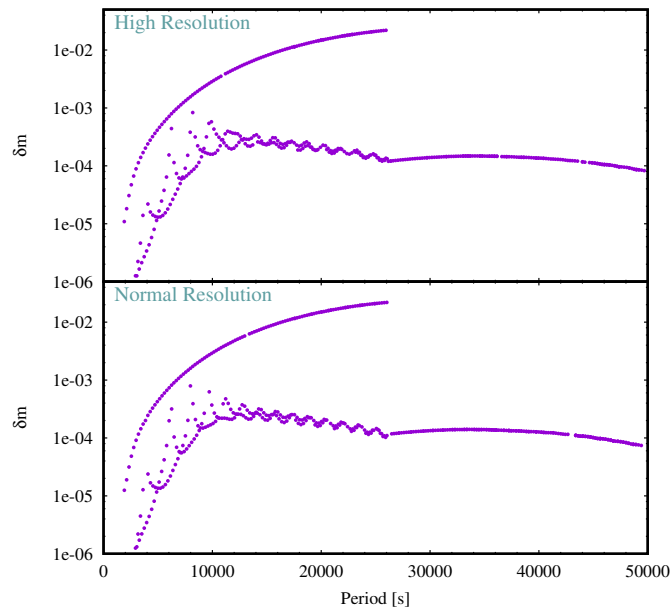


Figure 14: **Comparison of predicted amplitudes δm for DM models computed with different mesh resolutions.** The high resolution model was computed with 44374 mesh points and compared with the 13629 mesh points in the normal resolution run.

References

- [1] Schwarzschild, M. & Härm, R. Red Giants of Population II. II. *Astrophys. J.* **136**, 158 (1962).
- [2] Thomas, H.-C. Sternentwicklung VIII. Der Helium-Flash bei einem Stern von 1.3 Sonnenmassen. *ZAp* **67**, 420 (1967).
- [3] Sullivan, P. W. *et al.* The Transiting Exoplanet Survey Satellite: Simulations of Planet Detections and Astrophysical False Positives. *Astrophys. J.* **809**, 77 (2015).
- [4] Geier, S. *et al.* The catalogue of radial velocity variable hot subluminous stars from the MUCHFUSS project (Corrigendum). *Astron. Astrophys.* **602**, C2 (2017).
- [5] Randall, S. K., Bagnulo, S., Ziegerer, E., Geier, S. & Fontaine, G. The enigmatic He-sdB pulsator LS IV-14°116: new insights from the VLT. *Astron. Astrophys.* **576**, A65 (2015).
- [6] Østensen, R. H. *et al.* KIC 1718290: A Helium-rich V1093-Her-like Pulsator on the Blue Horizontal Branch. *Astrophys. J. Lett.* **753**, L17 (2012).
- [7] Jeffery, C. S. *et al.* Discovery of a variable lead-rich hot subdwarf: UVO 0825+15. *Mon. Not. R. Astron. Soc.* **465**, 3101–3124 (2017).
- [8] Latour, M., Green, E. M. & Fontaine, G. Discovery of a second pulsating intermediate helium-enriched sdOB star. *Astron. Astrophys.* **623**, L12 (2019).
- [9] Dorman, B., Rood, R. T. & O’Connell, R. W. Ultraviolet Radiation from Evolved Stellar Populations. I. Models. *Astrophys. J.* **419**, 596 (1993).
- [10] Kippenhahn, R., Weigert, A. & Weiss, A. *Stellar Structure and Evolution* (2012).
- [11] Battich, T., Miller Bertolami, M. M., Córscico, A. H. & Althaus, L. G. Pulsational instabilities driven by the ϵ mechanism in hot pre-horizontal branch stars. I. The hot-flasher scenario. *Astron. Astrophys.* **614**, A136 (2018).

- [12] Unno, W., Osaki, Y., Ando, H., Saio, H. & Shibahashi, H. *Nonradial oscillations of stars* (1989).
- [13] Cassisi, S. & Salaris, M. *Old Stellar Populations: How to Study the Fossil Record of Galaxy Formation* (2013).
- [14] Chaplin, W. J. *et al.* Ensemble Asteroseismology of Solar-Type Stars with the NASA Kepler Mission. *Science* **332**, 213 (2011).
- [15] Mosser, B. *et al.* Red-giant seismic properties analyzed with CoRoT. *Astron. Astrophys.* **517**, A22 (2010).
- [16] Beck, P. G. *et al.* Kepler Detected Gravity-Mode Period Spacings in a Red Giant Star. *Science* **332**, 205 (2011).
- [17] Bildsten, L., Paxton, B., Moore, K. & Macias, P. J. Acoustic Signatures of the Helium Core Flash. *Astrophys. J. Lett.* **744**, L6 (2012).
- [18] Deheuvels, S. & Belkacem, K. Seismic characterization of red giants going through the helium-core flash. *Astron. Astrophys.* **620**, A43 (2018).
- [19] Goldreich, P. & Kumar, P. Wave generation by turbulent convection. *Astrophys. J.* **363**, 694–704 (1990).
- [20] Shiode, J. H., Quataert, E., Cantiello, M. & Bildsten, L. The observational signatures of convectively excited gravity modes in main-sequence stars. *Mon. Not. R. Astron. Soc.* **430**, 1736–1745 (2013).
- [21] Heber, U. Hot Subluminous Stars. *Publ. Astron. Soc. Pacific* **128**, 082001 (2016).
- [22] Castellani, M. & Castellani, V. Mass Loss in Globular Cluster Red Giants: an Evolutionary Investigation. *Astrophys. J.* **407**, 649 (1993).
- [23] Brown, T. M., Sweigart, A. V., Lanz, T., Landsman, W. B. & Hubeny, I. Flash Mixing on the White Dwarf Cooling Curve: Understanding Hot Horizontal Branch Anomalies in NGC 2808. *Astrophys. J.* **562**, 368–393 (2001).
- [24] Cassisi, S., Schlattl, H., Salaris, M. & Weiss, A. First Full Evolutionary Computation of the Helium Flash-induced Mixing in Population II Stars. *Astrophys. J. Lett.* **582**, L43–L46 (2003).

- [25] Lanz, T., Brown, T. M., Sweigart, A. V., Hubeny, I. & Landsman, W. B. Flash Mixing on the White Dwarf Cooling Curve: Far Ultraviolet Spectroscopic Explorer Observations of Three He-rich sdB Stars. *Astrophys. J.* **602**, 342–355 (2004).
- [26] Miller Bertolami, M. M., Althaus, L. G., Unglaub, K. & Weiss, A. Modeling He-rich subdwarfs through the hot-flasher scenario. *Astron. Astrophys.* **491**, 253–265 (2008).
- [27] Tailo, M. *et al.* Rapidly rotating second-generation progenitors for the ‘blue hook’ stars of ω Centauri. *Nature* **523**, 318–321 (2015).
- [28] Córscico, A. H., Althaus, L. G. & Miller Bertolami, M. M. New nonadiabatic pulsation computations on full PG 1159 evolutionary models: the theoretical GW Virginis instability strip revisited. *Astron. Astrophys.* **458**, 259–267 (2006).
- [29] Lecoanet, D. & Quataert, E. Internal gravity wave excitation by turbulent convection. *Mon. Not. R. Astron. Soc.* **430**, 2363–2376 (2013).
- [30] Couston, L.-A., Lecoanet, D., Favier, B. & Le Bars, M. The energy flux spectrum of internal waves generated by turbulent convection. *Journal of Fluid Mechanics* **854**, R3 (2018).
- [31] Rogers, T. M., Lin, D. N. C., McElwaine, J. N. & Lau, H. H. B. Internal Gravity Waves in Massive Stars: Angular Momentum Transport. *Astrophys. J.* **772**, 21 (2013).
- [32] Miller Bertolami, M. M. New models for the evolution of post-asymptotic giant branch stars and central stars of planetary nebulae. *Astron. Astrophys.* **588**, A25 (2016).
- [33] Naslim, N., Jeffery, C. S., Ahmad, A., Behara, N. T. & Şahin, T. Abundance analyses of helium-rich subluminescent B stars. *Mon. Not. R. Astron. Soc.* **409**, 582–590 (2010).
- [34] Ahmad, A. & Jeffery, C. S. Discovery of pulsation in a helium-rich subdwarf B star. *Astron. Astrophys.* **437**, L51–L54 (2005).
- [35] Saio, H. & Jeffery, C. S. The excitation of g-mode pulsations in hot helium-rich subdwarfs. *Mon. Not. R. Astron. Soc.* **482**, 758–761 (2019).

- [36] Gesicki, K., Zijlstra, A. A. & Miller Bertolami, M. M. The mysterious age invariance of the planetary nebula luminosity function bright cut-off. *Nature Astronomy* **2**, 580–584 (2018).
- [37] Guerrero, M. A. *et al.* The inside-out planetary nebula around a born-again star. *Nature Astronomy* **2**, 784–789 (2018).
- [38] Vitense, E. Die Wasserstoffkonvektionszone der Sonne. Mit 11 Textabbildungen. *ZAp* **32**, 135 (1953).
- [39] Dziembowski, W. Light and radial velocity variations in a nonradially oscillating star. *Acta Astron.* **27**, 203–211 (1977).
- [40] Battich, T., Miller Bertolami, M. M., Córscico, A. H. & Althaus, L. G. Pulsational instabilities driven by the ϵ mechanism in hot pre-horizontal branch stars. I. The hot-flasher scenario. *Astron. Astrophys.* **614**, A136 (2018). .
- [41] Randall, S. K., Bagnulo, S., Ziegerer, E., Geier, S. & Fontaine, G. The enigmatic He-sdB pulsator LS IV-14°116: new insights from the VLT. *Astron. Astrophys.* **576**, A65 (2015).
- [42] Østensen, R. H. *et al.* KIC 1718290: A Helium-rich V1093-Her-like Pulsator on the Blue Horizontal Branch. *Astrophys. J. Lett.* **753**, L17 (2012).
- [43] Jeffery, C. S. *et al.* Discovery of a variable lead-rich hot subdwarf: UVO 0825+15. *Mon. Not. R. Astron. Soc.* **465**, 3101–3124 (2017).
- [44] Latour, M., Green, E. M. & Fontaine, G. Discovery of a second pulsating intermediate helium-enriched sdOB star. *Astron. Astrophys.* **623**, L12 (2019).
- [45] Unno, W., Osaki, Y., Ando, H., Saio, H. & Shibahashi, H. *Nonradial oscillations of stars* (1989).

Acknowledgements

This work was partially supported by ANPCyT through grant PICT 2016-0053, and by the MinCyT-DAAD bilateral cooperation program through

grant DA/16/07. Funding for the Stellar Astrophysics Centre is provided by The Danish National Research Foundation (Grant DNRF106). This research was supported in part by the National Science Foundation under Grant No. NSF PHY-1748958. M.M.M.B. gratefully acknowledges the financial support by the Stellar Astrophysics Centre (Denmark) that allowed him to participate in several Aarhus red giants challenge workshops where the central ideas of this paper were conceived.

Author informations

Affiliations

M. M. Miller Bertolami

Instituto de Astrofísica de La Plata, UNLP-CONICET,
Paseo del Bosque s/n, 1900 La Plata, Argentina;
e-mail: marcelo@mpa-garching.mpg.de

T. Battich

Instituto de Astrofísica de La Plata, UNLP-CONICET,
Paseo del Bosque s/n, 1900 La Plata, Argentina;
e-mail: tbattich@fcaglp.fcaglp.unlp.edu.ar

A. H. Córscico

Instituto de Astrofísica de La Plata, UNLP-CONICET,
Paseo del Bosque s/n, 1900 La Plata, Argentina;
e-mail: acorsico@fcaglp.fcaglp.unlp.edu.ar

J. Christensen-Dalsgaard

Stellar Astrophysics Centre, Department of Physics and Astronomy, Aarhus University,
Ny Munkegade 120, DK-8000 Aarhus C, Denmark;
Kavli Institute for Theoretical Physics, University of California Santa Barbara,
CA 93106-4030, USA;
e-mail: jcd@phys.au.dk

L. G. Althaus

Instituto de Astrofísica de La Plata, UNLP-CONICET,
Paseo del Bosque s/n, 1900 La Plata, Argentina;
e-mail: althaus@fcaglp.fcaglp.unlp.edu.ar

Contributions

M.M.M.B. developed the idea, derived the theoretical expressions and performed the pulsation computations. T.B. derived the theoretical expressions and computed the stellar models with `LPCODE`. A.H.G. programed LP-PUL and discussed the modelling of stochastic excitation. J.C.D. provided insight in the nature of stochastic oscillations and the modelling of stochastic excitation. All authors participated in discussions of the results, their presentations in figures and descriptions in the manuscript and in pinpointing the conclusions.

Competing interests

The authors declare no competing financial interests.

Corresponding author

M. M. Miller Bertolami